

Critical asymmetry and the systematics of fission-like processes in the reactions of ^{12}C projectiles with medium mass nuclei*

J. B. Natowitz, M. N. Namboodiri, and E. T. Chulick†

Cyclotron Institute and Department of Chemistry, Texas A & M University, College Station, Texas 77843

(Received 24 July 1975)

The systematics of fission-like processes observed in reactions induced by 107- and 197-MeV ^{12}C projectiles have been investigated. Counter telescopes were employed to detect and identify the products of reactions with ^{89}Y , ^{98}Mo , Ag, and ^{116}Sn . Limited experiments using Ni and Au targets were also performed. For the medium mass targets, cross sections, energy distributions, and angular distributions of the reaction products are reported. Limiting angular momenta for the fusion of ^{12}C with Y, Mo, and Ag have been determined and are used to estimate the angular momenta of the collisions leading to fission-like reactions. The probability of occurrence of such reactions is compared with predictions based upon the concept of an angular momentum dependent critical asymmetry. This concept is found to be very useful in discussing the reaction mechanisms involved.

[NUCLEAR REACTIONS Ni, ^{89}Y , ^{98}Mo , Ag, ^{116}Sn , $^{197}\text{Au}(^{12}\text{C}, x)$, $E=107, 197$ MeV; measured absolute $\sigma(\theta)$, σ and \bar{E} for fission-like products.]

INTRODUCTION

The availability of heavy ion projectiles of higher energy and higher mass has led to a renewed interest in studying the interactions of two large pieces of nuclear matter. Recent experimental results¹⁻³ have re-emphasized earlier indications⁴⁻⁶ that the reaction mechanisms possible in such interactions cannot be simply divided into fast direct processes and slow compound nucleus processes. Instead it appears that processes occurring over the entire reaction time span from direct to compound reactions can be observed with significant probabilities.

The systematic experimental and theoretical investigation of these interactions, sometimes called nuclear macrophysics, has considerable overlap with studies of the fission process and is already providing new insights into the properties of nuclear matter. In this paper we report studies of the reactions of ^{12}C projectiles, primarily with target nuclei of medium mass. Fusion, fission, and intermediate fission-like reactions were studied. The results are discussed in terms of the concept of critical asymmetry⁷ with emphasis upon the effect of angular momentum on the nuclear potential energy surface.

EXPERIMENTS

The products of the reactions of ^{12}C projectiles with various target nuclei were detected using semiconductor detector telescopes. These telescopes typically consisted of three detectors. For most experiments, the front detector was a totally depleted 8.4- μm -thick detector. In some experi-

ments that front detector was replaced by a totally depleted 4.3- μm -thick detector. Both detectors were too thin to allow isotopic resolution but permitted elemental resolution. The second detector was typically 50 to 100 μm thick and the third detector was 1 to 2 mm thick. Since the products of interest in these studies ordinarily stopped in the second detector, the third detector served primarily as a reject detector, eliminating light particles from the particle spectra.

The detectors were calibrated using 5.486-MeV α particles from a ^{241}Am source. The reactions of 107-MeV and 197-MeV ^{12}C projectiles were studied. Targets were Ni (300 $\mu\text{g}/\text{cm}^2$), ^{89}Y (970 $\mu\text{g}/\text{cm}^2$), ^{98}Mo (554 $\mu\text{g}/\text{cm}^2$), Ag (550 $\mu\text{g}/\text{cm}^2$), ^{116}Sn (200 $\mu\text{g}/\text{cm}^2$), and ^{197}Au (274 $\mu\text{g}/\text{cm}^2$). Only a limited number of experiments were performed using the Ni and Au targets since the emphasis in this work was on the study on the reactions with medium mass target nuclei having mass ≈ 100 amu.

During an irradiation, the detector telescope data were recorded event by event on magnetic tape for later off-line processing. This processing was accomplished with the computer code DINIT (see Ref. 8) which, in its current version, employs a table look-up technique to assign particle identification (PI) values to the detected ions. The identification tables are initially based upon the semi-empirical range-energy calculations of Northcliffe and Schilling⁹ but have been modified to take into account pulse height defects and detector window effects. The data required to make these modifications were obtained by comparing the measured detector telescope energies of ^{14}N , ^{16}O , ^{28}Si , ^{40}Ar , ^{56}Fe , and ^{84}Kr ions, accelerated in the TAMU

Variable Energy Cyclotron, with the energies determined by magnetic analysis of the ion beam.

Table entries consist of the atomic number of ions along the line of β stability as a function of the apparent total energy, E_T , and of the apparent fractional energy loss in the ΔE detector, $\Delta E/E_T$. While the pulse height defect data could be employed to correct the observed energies, thus allowing us to construct a table of actual E_T vs the actual fractional energy loss, the use of such a table for identification purposes would require some prior knowledge of the particle identity or alternatively, an iterative procedure involving more than one entry into the identification table. To reduce the time required for the identification, we have chosen to use an empirical table of apparent E_T and $\Delta E/E_T$, making energy corrections after the identification is completed.

The identification scheme consists of the following:

1. employing the detector energy calibrations to calculate the energies in the individual detector,
2. separating the events into two detector events and three detector events,
3. calculating the total energy E_T and the fractional energy loss $\Delta E/E_T$, in the front detector (or front two detectors for three-detector events),
4. searching a table of $\Delta E/E_T$ vs E_T to assign a PI value to the event,
5. correcting the observed energies for pulse height defect and energy loss in the target.

The first correction is made using the formulation proposed by Kaufmann *et al.*¹⁰ with the constant A of the correction equation [Eq. (5) of Ref. 10] determined to be 17.0 from our pulse height defect data. The correction for average energy loss in the target is made using range-energy information⁹ to calculate the energy loss of the ion in an amount of target material equal to one-half the target thickness corrected for the angle of observation. Since the table is constructed from range energy information for nuclei along the line of β stability, the PI values are close to but not necessarily equal to the atomic number of the detected product.

Once the energies and PI values have been determined, the events may be combined to construct the various PI and energy spectra as desired.

RESULTS

The general features of the data which we obtain with the counter telescopes are well illustrated in Fig. 1 which depicts the variation of ΔE with E for the reactions of 197-MeV ^{12}C with Ag. The ridge of products of intermediate ΔE having a relatively narrow spread in total energy are those which are

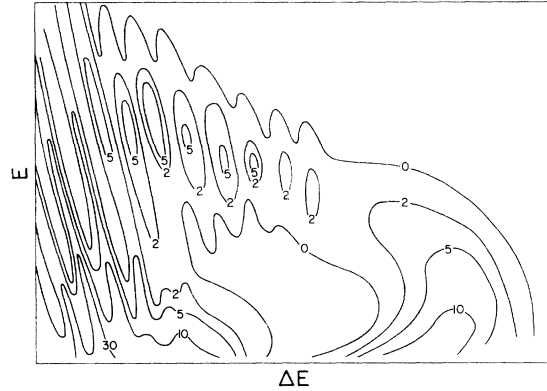


FIG. 1. Spectrum of ΔE vs E for products of the reactions of 197-MeV ^{12}C with Ag. Data are for elements detected at a laboratory angle of 40° with a telescope employing an $8.4\text{-}\mu\text{m}$ -thick ΔE detector.

of primary interest in this study. Products of higher Z , corresponding to the lower energy heavy recoils from fusion reactions, are mostly stopped in the ΔE detector and are not identified, which results in the sharp energy cutoff observed in the figure for products of the highest ΔE .

Even though the ΔE detectors stop the majority of the recoils from fusion, the total cross sections for production of nonfissioning fusion residues have been measured for the reactions of 197-MeV ^{12}C projectiles with ^{89}Y , ^{98}Mo , and Ag targets. These measurements were performed by combining the cross sections for transmitted heavy recoils with the measured cross sections for heavy recoils stopped in the $4.3\text{-}\mu\text{m}$ ΔE detector. Determination of the latter cross section was possible because the particles of much lower Z than the fusion residues can leave very little energy in the thin detector. As a result, the energy spectrum of stopped recoils is quite distinct from the lower energy pulses corresponding to lighter ions. The cross sections for fusion not followed by fission are presented in Table I.

In Fig. 2, we show particle identified spectra derived from ΔE versus E data such as that shown

TABLE I. Limiting angular momenta for the production of heavy recoils in reactions with 197-MeV ^{12}C projectiles.

Target	Compound Nucleus	Cross section (mb)	Sharp cutoff limiting angular momentum (\hbar)
^{89}Y	^{101}Rh	1770 ± 180	70 ± 4
^{98}Mo	^{110}Cd	1910 ± 195	74 ± 4
Ag	^{120}I	1810 ± 185	73 ± 4

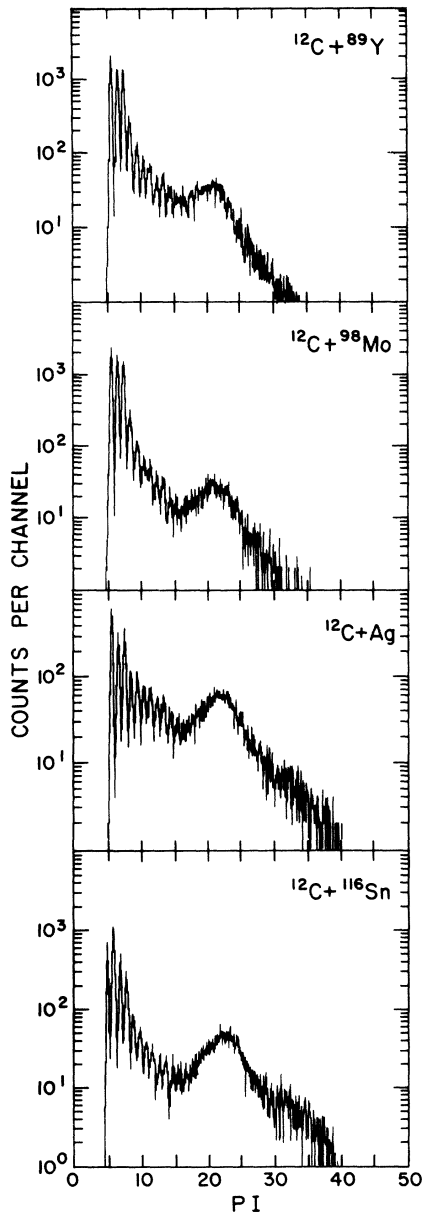


FIG. 2. Identified spectra for products of the reactions of 197-MeV ^{12}C projectiles with ^{89}Y , ^{98}Mo , Ag, and ^{116}Sn . Data are for elements detected at a laboratory angle of 40° with a telescope employing an $8.4\text{-}\mu\text{m}$ -thick ΔE detector. The highest peak in each spectrum represents carbon ions. The PI values are assigned using an identification table based on semiempirical range energy calculations (see text).

in Fig. 1 for the Ag target. The elemental resolution obtained using the $8.4\text{-}\mu\text{m}$ ΔE detector is found to be adequate to separate elements up to $Z \approx 16$. Above that atomic number, only the envelope of the elemental product yield is observed. When elements are resolved the correspondence between

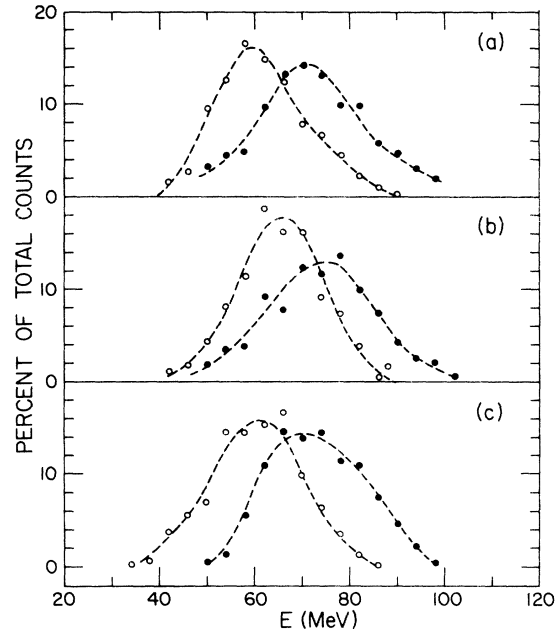


FIG. 3. Representative laboratory energy spectra for elements produced in the reactions of 197-MeV ^{12}C with Ag. Data were taken at laboratory angles of 35° (\bullet) and 50° (\circ). Spectra are shown for (a) Mg ions, (b) S ions, and (c) Ca ions.

PI and atomic number is well established. For higher atomic numbers we rely on our calibration procedures to establish this correspondence. As the atomic number of the product becomes greater than 20, there does appear to be a systematic deviation of PI from Z in our data. The deviation is such that the actual atomic number corresponding to the peak at symmetry may be 1 to 2 atomic numbers higher than would be indicated by equating PI to Z . We have attempted to correct for this effect in assigning counts to bins of a particular atomic number, above the point where elements are clearly resolved. This slight uncertainty at high atomic number has little effect on the conclusions of this paper.

By the assignment of appropriate windows in the PI spectrum, energy spectra of the individual elements may be obtained. Figure 3 illustrates the nature of the typical energy spectra observed for the reaction products of atomic number intermediate between that of the projectile and the composite system. These energy spectra are characteristically relatively narrow, almost symmetric distributions with peak energies which decrease rapidly with increasing laboratory angles.

The high average energies and narrow energy distributions observed for products of atomic number ranging from those slightly greater than that

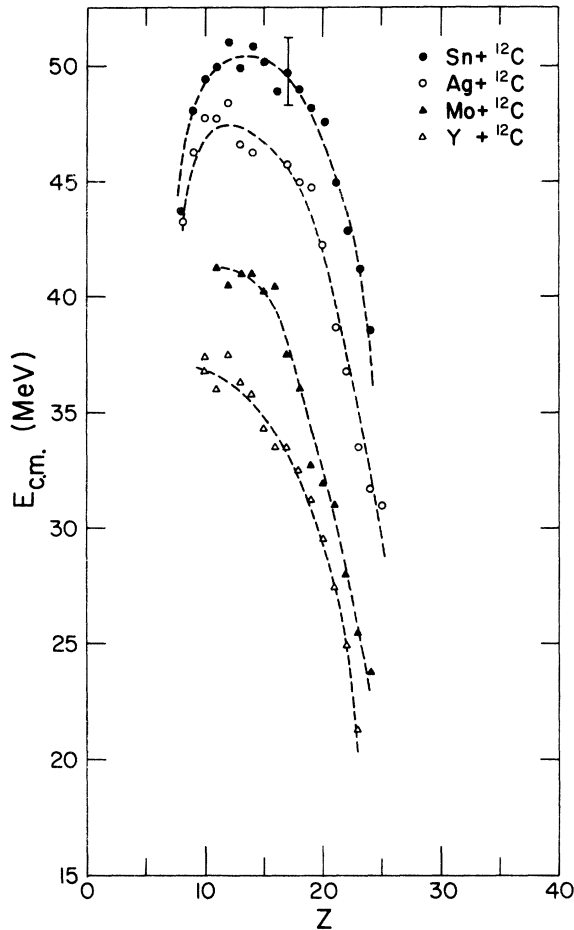


FIG. 4. Variation of peak energies with atomic number for products of the reactions of ^{12}C with ^{89}Y (Δ), ^{88}Mo (\blacktriangle), Ag (\circ); and ^{116}Sn (\bullet). The data have been converted to the center of mass assuming two-body breakup. The estimated uncertainty of ± 1.5 MeV is indicated by the error bar.

of the projectile into the region of atomic numbers corresponding to symmetric fission suggest that these products result from a process which is predominantly a two-body breakup. That such is the case has been confirmed by coincidence experiments, employing two counter telescopes, which will be reported elsewhere.¹¹ For the present, we shall refer to such reactions as "fission-like processes."

In order to explore the systematics of the energies more carefully, we have converted the observed peak energies in the laboratory to center of mass energies by assuming that the observed products result from a binary division of the composite system formed by the target and projectile nuclei. In making these conversions we have not taken any product excitation energy, and therefore any mass decrease of the products after division,

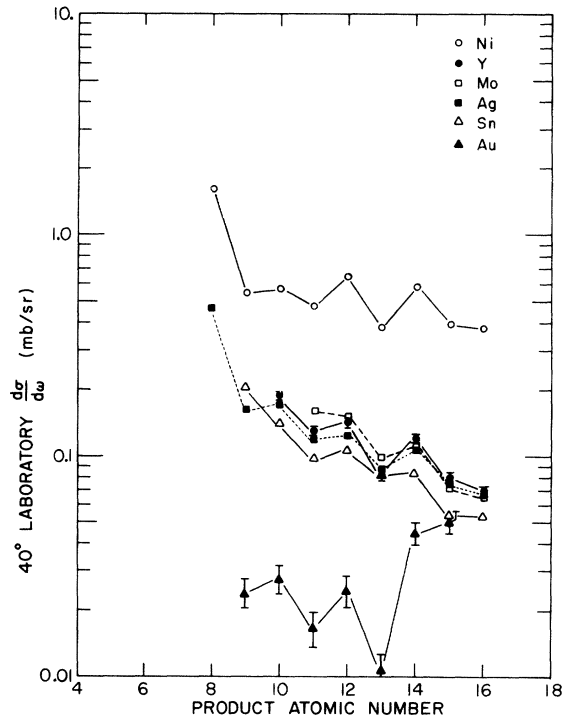


FIG. 5. Target-mass dependence of the cross sections for light fission-like products. The differential cross sections ($d\sigma/d\omega$) for elements detected at 40° are plotted for the reactions of 197-MeV ^{12}C projectiles with Ni (\circ), Y (\bullet), Mo (\square), Ag (\blacksquare), Sn (\triangle), and Au (\blacktriangle). An interesting odd-even alternation is observed.

into account.

When such conversions are made for the energy data obtained at laboratory angles of 20° to 80° in the reactions of ^{12}C projectiles with the ^{89}Y , ^{88}Mo , Ag , ^{116}Sn , and ^{197}Au targets the resultant center of mass energies for each product vary with target mass but for each target are constant with angle within the experimental error of ± 1.5 MeV. Within the same experimental error, no systematic difference in the center of mass energies was observed in experiments with lower energy projectiles. In the limited experiments with Ni targets it appeared that the center of mass energies do vary with angle of emission. The Ni + ^{12}C system is being investigated further.

In Fig. 4 the peak energies converted to the center of mass are plotted as a function of the atomic number of the product.

The cross sections for the products having the characteristic energy spectra of the type illustrated in Fig. 3 have also been measured. An indication of the variation of the cross section for such processes with mass of the target nucleus is indicated in Fig. 5. This plot is one of differential cross sections for various elements detected at 40° in the laboratory. The sharp decline in the

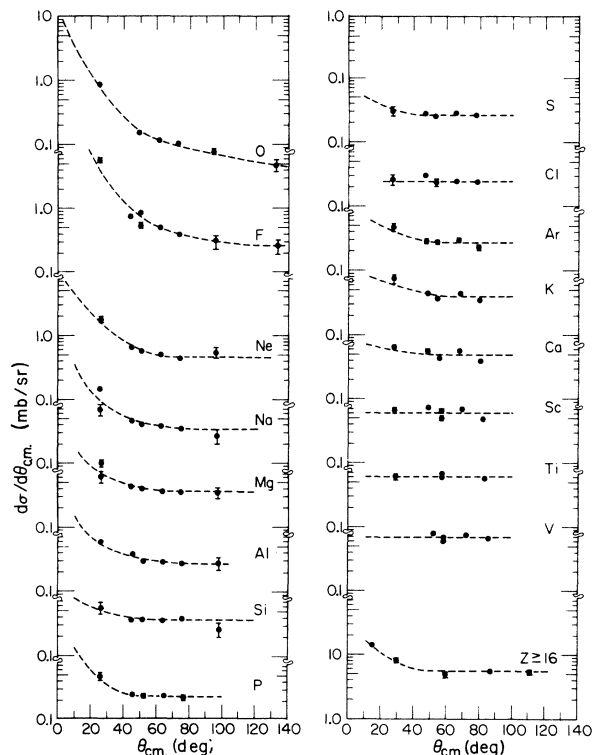


FIG. 6. Center of mass angular distributions $d\sigma/d\theta_{c.m.}$ for elements produced in fission-like reactions of 197-MeV ^{12}C projectiles with Ag. The forward peaking decreases as the atomic number of the detected product increases. The apparently constant value of $d\sigma/d\theta$ which is observed at the larger angles corresponds to a $1/\sin\theta$ angular dependence for $d\sigma/d\omega$. Uncertainties are of the order of the size of the solid circles unless otherwise indicated.

cross sections of elements of atomic number in the range of $Z = 8$ to 16 as the target mass increases is readily observed. The odd-even variation in the yield data at lower atomic number is similar to that previously observed.³

For the medium mass elements, angular distributions of the products of fission-like reactions have been obtained. The data for the reactions of Ag with ^{12}C , presented in Fig. 6, are representative of these data. Here the differential cross sections $d\sigma/d\theta_{c.m.}$ are plotted as a function of center of mass angle. We choose this way of plotting the data since a horizontal line corresponding to constant $d\sigma/d\theta_{c.m.}$ would be indicative of a variation of $d\sigma/d\omega_{c.m.}$ of the form $1/\sin\theta$. The angular distributions for the products of fission-like processes indicate a continuous trend towards the limiting $1/\sin\theta$ variation¹² of $d\sigma/d\omega$ as the atomic number of the product increases above that of the projectile. However, even products with atomic

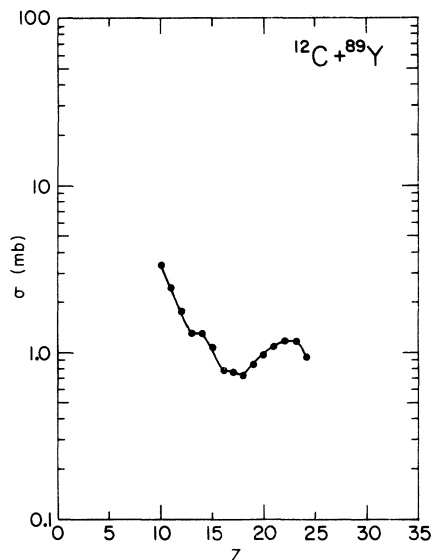


FIG. 7. Elemental yields of the products of the fission-like reactions of ^{12}C projectiles with ^{89}Y . The data are for a projectile energy of 197 MeV. The estimated absolute error is $\pm 10\%$.

number well above that of the projectile exhibit a small forward peaking in their angular distribution.

By integrating over the angular distributions, we have determined the elemental yields which are presented in Figs. 7-10. Extrapolations of $d\sigma/$

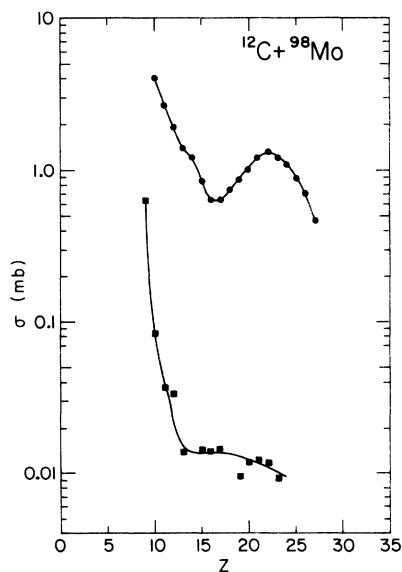


FIG. 8. Elemental yields of the products of the fission-like reactions of ^{12}C projectiles with ^{98}Mo . The data are for projectile energies of 107 MeV (■) and 197 MeV (●). The estimated absolute error is $\pm 10\%$.

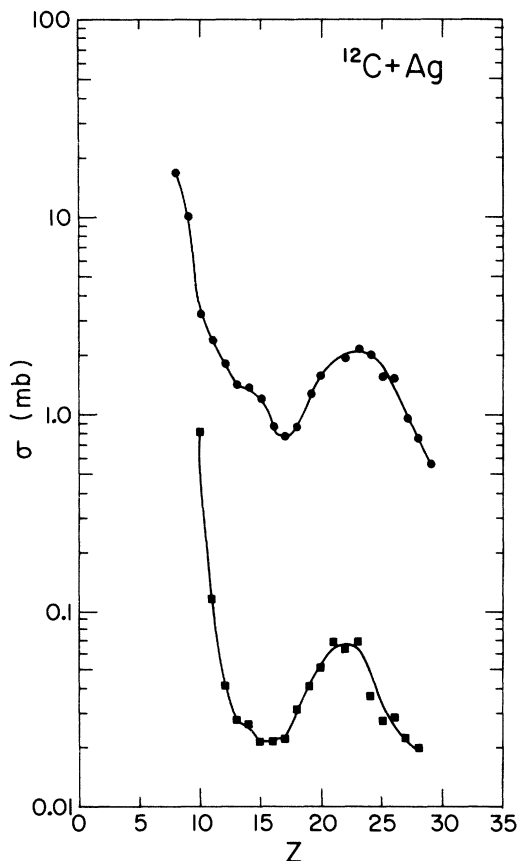


FIG. 9. Elemental yields of the products of the fission-like reactions of ^{12}C projectiles with Ag. The data are for projectile energies of 107 MeV (■) and 197 MeV (●). The estimated absolute error is $\pm 10\%$.

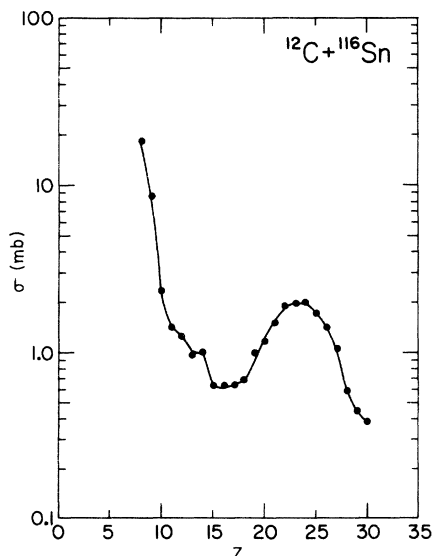


FIG. 10. Elemental yields of the products of the fission-like reactions of ^{12}C projectiles with ^{116}Sn . The data are for a projectile energy of 197 MeV. The estimated absolute error is $\pm 10\%$.

$d\theta_{\text{c.m.}}$ at large c.m. angles were made for this purpose.

DISCUSSION

In a system in which reaction mechanisms can be clearly separated into two distinct types, fast and slow, product angular distributions varying essentially as $1/\sin\theta$ but having a forward peaking would suggest the existence of both reaction mechanisms leading to those particular final products. However, the smooth continuous variation of the yields of the products, their peak energies and their angular distributions as indicated in the figures, are more suggestive of a continuous evolution of the reaction system³ rather than a synthesis of two distinct processes. In the reactions under consideration here, the tendency toward the limiting $1/\sin\theta$ dependence for the angular distribution probably reflects the requirement that the reactions for which large amounts of mass transfer occur proceed through the production of an intermediate composite nucleus which exists for a time long compared to the rotational time. Such a composite nucleus would not necessarily be a compound nucleus in the same sense as it is usually defined. Although there may well be dynamic equilibration achieved in most of the degrees of freedom, the system does retain some additional memory of the formation step in its elongation and asymmetry.

Within the framework of the macroscopic approach, a complete description of the interactions between two large nuclei must necessarily take into account the potential energy surface as a function of all of the pertinent degrees of freedom and the dynamic path of the system on that potential energy surface. Swiatecki has estimated¹³ that specification of approximately 14 degrees of freedom would be required to (completely) describe a binary process such as fusion or fission and that "three degrees of freedom is the barest minimum necessary to give the roughest, qualitatively adequate description of the nuclear shapes relevant for binary fission or two-ion fusion."

The minimum three degrees of freedom suggested by Swiatecki are

- α_2 , a separation coordinate,
- α_3 , a mass asymmetry coordinate,
- α_4 , a neck forming coordinate.

Figure 11, an illustration of the fission and fusion shapes described by the coordinates α_2 and α_4 for a fixed value of the asymmetry coordinate, α_3 , is similar to that presented by Swiatecki. This figure emphasizes an important feature of the nuclear potential energy surface in $\alpha_2, \alpha_3, \alpha_4$ space,

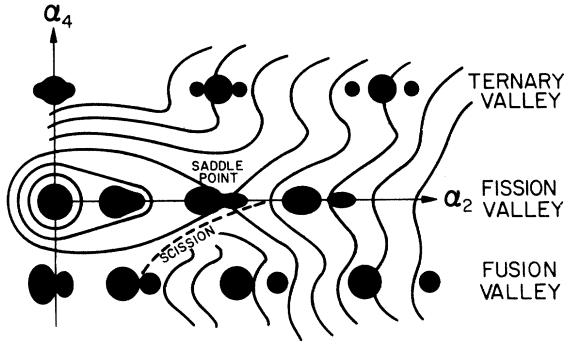


FIG. 11. Schematic representation of the potential surface in the α_2 - α_4 plane for a constant value of the asymmetry coordinate, α_3 . The diagram indicates shapes representative of the reactions of ^{12}C nuclei with medium mass target nuclei.

the misalignment of the fusion and fission valleys, reflecting the very different shapes of the nuclei in the two different processes.

In reactions with relatively light projectiles on heavy targets, fission has been well described as a statistical process competing with other possible modes of deexcitation of a compound nucleus and totally independent of the fusion step. This clear separation between fusion and fission may be viewed as a consequence of the asymmetric nature of the initial collision resulting in a complete absorption of the projectile and producing a composite nuclear shape more compact than the symmetric saddle point shape of the fissioning compound nucleus. For projectiles of significantly greater mass, nuclear charge, or orbital angular momentum, the very different nuclear potential in α_2 , α_3 , α_4 space and the increased importance of dynamic effects can greatly alter the nature of the interaction.¹⁻⁶

CRITICAL ASYMMETRY

While various approaches to full dynamic treatments of the interaction between complex nuclei are being developed,^{14,15} at this time no complete dynamic calculations encompassing the wide variety of reactions possible in the evolving system are yet available. However, just as it is possible to gain considerable insight into the nature of the fusion and fission processes by focusing on the potential energy variation in the single α_2 degrees of freedom,^{16,17} it appears possible to understand the basic features of collisions with large kinetic energy damping by considering that degree of freedom which is expected to be of primary importance at some decisive stage of the interaction. In this spirit, we focus our attention on the asymmetry coordinate, α_3 .

For the case of zero angular momentum, Swiatecki⁷ has estimated the critical asymmetry of a saddle point nucleus as a function of the nuclear fissionability and has emphasized the importance of the critical asymmetry in determining the qualitative nature of the interaction between two complex nuclei. For a particular fissionability, a nucleus having a shape more asymmetric than that characterized by the critical asymmetry would be unstable toward asymmetric distortions, a nucleus having a shape more symmetric than that characterized by the critical asymmetry would be stable towards such distortions.

As a result, for mass asymmetries more extreme than the critical asymmetry, the smaller portion of an asymmetric nucleus would be preferentially absorbed into the larger portion. For mass asymmetries less extreme than the critical asymmetry, the smaller portion would grow, drawing mass from the larger portion, the entire system thus evolving toward a symmetric mass distribution.

The value of the fissionability parameter, X [see Eq. (2)], below which a symmetric saddle point shape is unstable toward asymmetric distortions, is known as the Businaro-Gallone limit.¹⁸ At zero angular momentum, this limit has a value $X = 0.396$ (see Ref. 19) corresponding to nuclei in the vicinity of $Z = 44$. The variation of the Businaro-Gallone limit with angular momentum has been calculated for symmetric saddle point shapes,¹⁹ but no general calculations of the critical asymmetry as a function of angular momentum and fissionability have been reported.

In view of the misalignment of the fusion and fission valleys and the absence of any experimental evidence for large distortions of colliding complex nuclei, the critical asymmetries most pertinent to determining the probability of fission-like reactions may well be those appropriate to the nuclear shapes encountered in the fusion valley.

Moretto *et al.*³ have used a model of two rigidly rotating tangent spheres to calculate the potential energy of a composite system as a function of the asymmetry. We have employed a similar model, with the addition of a nuclear surface interaction of the form suggested by Krappe and Nix,²⁰ to make similar calculations. In our calculation, the energy of two tangent spherical nuclei relative to a spherical nucleus of the same total mass and charge is

$$V = E_{S_1} + E_{S_2} + E_{C_1} + E_{C_2} - E_{S_{CN}} - E_{C_{CN}} - E_{R_{CN}} + \frac{f\hbar^2 l(l+1)}{2\mu R^2} + \frac{z_1 z_2 e^2}{R} + V_{KN}. \quad (1)$$

In this equation, the numbers 1 and 2 indicate the

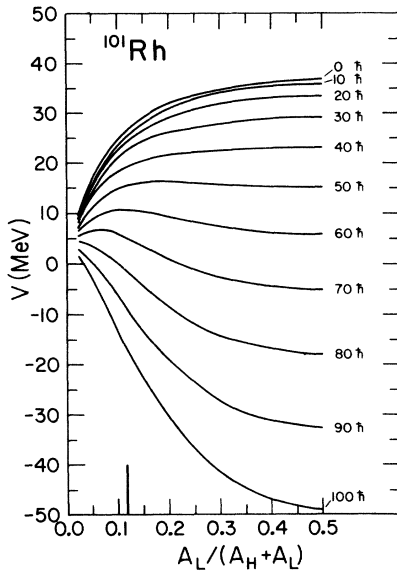


FIG. 12. Potential energy as a function of asymmetry for the composite system ^{101}Rh . The potential energy of two rigidly rotating tangent spheres has been calculated using Eq. (1) in the text. Increasing angular momentum stabilizes the symmetric configuration. The peak in the potential curve for a fixed angular momentum occurs at the critical asymmetry corresponding to that angular momentum. The initial asymmetry for $^{12}\text{C} + ^{89}\text{Y}$ is indicated by the heavy vertical line on the asymmetry scale.

two tangent nuclei and CN indicates the composite nucleus of the same total mass and atomic number. The energies designated E_S are surface energies, while those designated E_C are Coulomb energies. The rotational energy of the composite nucleus is $E_{R_{CN}}$. In the remaining terms of Eq. (1), l is the angular momentum quantum number, μ is the reduced mass, R is the separation distance of the spheres, ze is the nuclear charge. The symbol f is the factor which corrects for the variation of the moment of inertia of the rigidly rotating system as the asymmetry of the system varies.¹⁷ The final symbol V_{KN} represents the Knappe-Nix surface interaction. We have used a range of 1.35 fm in calculating that interaction. Other parameters employed in the calculation are identical with those of Ref. 19.

In Figs. 12 and 13, we show calculations of the potential energies for the composite systems ^{101}Rh and ^{120}I , two systems studied in the present work. In both cases, the symmetric configuration is unstable toward asymmetric distortions for zero angular momentum indicating that the point in the fusion valley at which the symmetric shape becomes stable toward asymmetric distortion occurs at a larger value of the fissionability parameter,

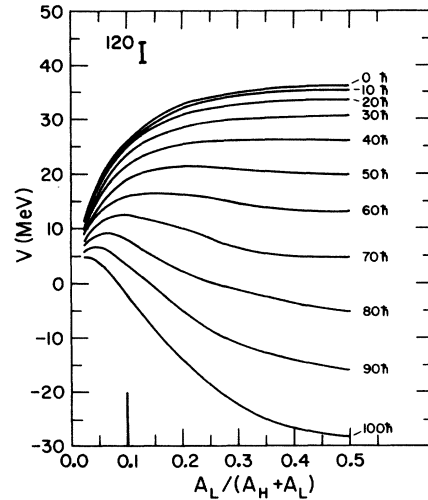


FIG. 13. Potential energy as a function of asymmetry for the composite system ^{120}I . The potential energy of two rigidly rotating tangent spheres has been calculated using Eq. (1) in the text. Increasing angular momentum stabilizes the symmetric configuration. The peak in the potential curve for a fixed angular momentum occurs at the critical asymmetry corresponding to that angular momentum. The initial asymmetry for $^{12}\text{C} + ^{108}\text{Ag}$ is indicated by the heavy vertical line on the asymmetry scale.

X , than the analogous Businaro-Gallone point in the fission valley.

As the angular momentum is increased, the slopes of the potential curves near symmetry decrease. At an angular momentum $\approx 45\hbar$ the symmetric shape becomes stable toward asymmetric distortions. The critical asymmetry, the point at which the potential curve peaks as a function of asymmetry, decreases rapidly with increasing angular momentum. The initial asymmetry of the two-sphere shape for a composite system prepared using ^{12}C projectiles is indicated on the abscissa in each figure. The critical asymmetries become less than these initial asymmetries for angular momenta $\approx 70\hbar$.

Composite systems of ^{101}Rh or ^{120}I having shapes more asymmetric than the critical asymmetry are expected to be unstable toward asymmetric distortions. In such cases, the smaller portion of the composite system should be absorbed into the larger portion. The system is expected to move toward fusion. In contrast, composite nuclei with asymmetries such that they are more symmetric than the shapes of critical asymmetry should show an initial predilection for evolving into a more symmetric shape. In this latter case, fission-like processes resulting from dynamic trajectories from the fusion valley to the fission valley without ever passing within the symmetric fission saddle

point in $\alpha_2, \alpha_3, \alpha_4$ space should be significantly enhanced.

The data on limiting angular momenta which we have derived²¹ from the cross sections for the production of nonfissioning heavy recoil nuclei allow us to make a more quantitative comparison of the probability of fission-like processes with the calculation. As indicated in Table I, the limiting angular momenta for fusion without fission in the reactions of 197-MeV ^{12}C projectiles with ^{89}Y , ^{98}Mo , and Ag are $70\hbar$, $74\hbar$, and $73\hbar$, respectively. It seems reasonable to assume that the reactions occurring for orbital angular momenta just above the limiting angular momenta for making nonfissioning nuclei are those which may lead to the fission-like reactions under consideration. Thus, for a projectile energy of 197 MeV, these angular momenta are seen to be slightly larger than the angular momentum at which the critical asymmetry in the fusion valley becomes less than the initial asymmetry. A significant probability of fission-like processes would therefore be expected.

We have not measured the fusion cross sections at the lower projectile energies. Based upon the systematics of previous measurements and the good agreement²¹ between the trend of the experimental limiting angular momenta and those calculated using the model proposed in Ref. 17, we estimate that the limiting angular momenta for production of ^{101}Rh , ^{110}Cd , and ^{120}I with 107-MeV ^{12}C projectiles are each $\approx 49\hbar$. As indicated in Figs. 12 and 13, $49\hbar$ is very close to the angular momentum above which the asymmetric shapes for these composite nuclei first become unstable relative to the symmetric shape. The fission-like processes are indeed observed at the lower projectile

energy but the cross sections are only 3% as large as the cross sections measured when higher energy projectiles are used.

It appears that the pronounced increase in fission-like processes as the kinetic energy of the ^{12}C projectiles is increased can be interpreted in terms of Figs. 12 and 13 as resulting from collisions involving angular momenta large enough that the symmetric shape of the composite system has been stabilized relative to asymmetric distortions.

Using the same model, we have calculated, as a function of fissionability, the variation of the critical asymmetry with angular momentum. The results are presented in Fig. 14. This figure is presented in terms of the two dimensionless parameters $X = E_C/2E_S$ and $Y = E_R/E_S$ where the energies E_S , E_C , and E_R are the surface, Coulomb, and rotational energies of the spherical composite nucleus.

Using the parameters of Ref. 19.

$$x = \frac{1}{50.883(1 - 1.7826I^2)} \frac{Z^2}{A}, \quad (2)$$

$$y = \frac{1.9249}{(1 - 1.7826I^2)} \frac{I^2}{A^{7/3}}, \quad (3)$$

and $I = (N - Z)/A$, where A , N , and Z are the mass number, neutron number, and atomic number of the nucleus, respectively.

For a particular value of the fissionability, the value of Y for which the critical asymmetry equals 0.5 corresponds to the angular momentum below which the symmetric shape is unstable with respect to asymmetric distortions. As indicated in our previous discussion the model predicts that the fission-like reactions should first become likely for that angular momentum. For higher angular momenta, the critical asymmetry for that same value of the fissionability is decreased. The value of Y at which the critical asymmetry becomes lower than the initial asymmetry of the system corresponds to the angular momentum for which fission-like reactions should be quite probable.

For comparison with the calculation, we have also plotted in Fig. 14 the initial asymmetries associated with the use of the particular projectiles ^4He , ^{12}C , ^{40}Ar , and ^{84}Kr to prepare nuclei of various fissionabilities. For a particular projectile, composite nuclei having values of Y above the dashed line in the figure are expected to evolve toward the spherical compound nucleus, while those with Y values below the line are expected to evolve toward two equal tangent spheres. The large enhancement of fission-like processes with increasing projectile mass, which has recently been observed,¹ is consistent with the qualitative predictions which would be made using Fig. 14.

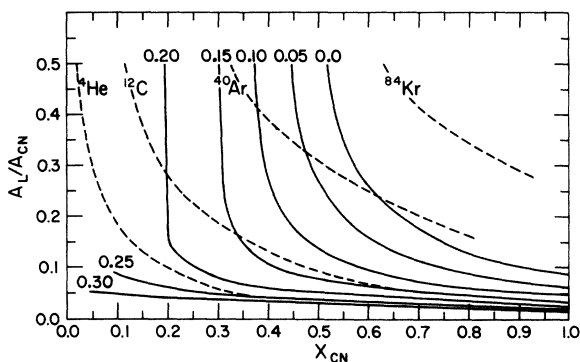


FIG. 14. Critical asymmetry as a function of fissionability and angular momentum. The critical asymmetries corresponding to fixed values of the parameter, $Y = E_R/E_S$, are plotted as a function of the fissionability parameter, $X = 2E_C/E_S$. Dashed lines indicate the initial asymmetries for reactions induced by ^4He , ^{12}C , ^{40}Ar , and ^{84}Kr projectiles (see text).

LIMITATIONS TO COMPOUND NUCLEUS FISSION

Angular distributions in the center of mass which are symmetric and tend toward the limiting $1/\sin\theta$ dependence expected for high angular momenta¹² are often taken as evidence supporting the formation of a compound nucleus, i.e., a completely equilibrated nucleus with a memory of the formation process limited to the information such as that contained in the distributions of excitation energy and angular momentum which result from a particular formation process. While such a symmetric angular distribution in the center of mass is not sufficient evidence of the existence of a compound nucleus, it is a necessary manifestation of the decay of a compound nucleus. We may, therefore, interpret the apparent constant values of $d\sigma/d\theta$, observed at the larger c.m. angles, as representing upper limits to the cross sections for production of the identified products in the decay of a compound nucleus. From plots such as Fig. 6, the limiting values of $d\sigma/d\theta$, and therefore the limiting yields corresponding to a compound nucleus mechanism, may be obtained. These limiting yields for the products of the reactions with 197-MeV ¹²C projectiles are presented in Fig. 15.

The odd-even variation of the yield noted in Fig. 5 is again apparent in the data in Fig. 15 although not in the total yield data of Figs. 7-10. This suggests that the variation reflects primarily the evaporative deexcitation of the excited nuclei following the initial collision.

Another interesting feature of the data is the fact that the limiting cross sections for products of atomic number ≤ 16 decrease slightly as the composite system varies from ¹⁰¹Rh to ¹²⁸Ba while the yields of the higher Z products, corresponding to symmetric division, increase by a factor of two. If in fact the product yields represented in Fig. 15 did result from the deexcitation of a true compound nucleus via the fission channel, this variation of the observed yield distributions would indicate an increasing importance of asymmetric fission as the mass of the compound nucleus decreased, in agreement with the behavior predicted to occur in the vicinity of the Businaro-Gallone limit.²²

However, since the Businaro-Gallone limit is a function of angular momentum,¹⁹ decreasing the projectile energy and, as a result, the angular momentum of the fissioning nuclei, should bring the shapes of these fissioning nuclei closer to the limiting shape, increasing the asymmetry of the distribution. This might explain the variation with projectile energy which is observed for the ¹¹⁰Cd system ($\alpha = 0.424$) in Fig. 8. The same trend is not apparent in Fig. 9 for ¹²⁰I ($\alpha = 0.472$).

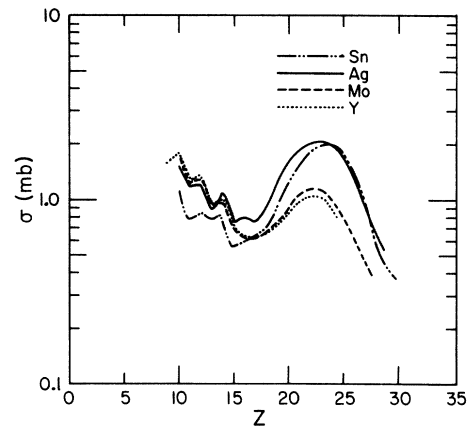


FIG. 15. Limits to the production of elements in fission-like reactions proceeding via a compound nucleus mechanism. The cross sections represent integration over angular distributions corresponding to a constant value of $d\sigma/d\theta_{c.m.}$. The data are for the reactions of 197-MeV ¹²C projectiles with ⁸⁹Y (dotted line), ⁸⁸Mo (dashed line), Ag (solid line), and ¹¹⁶Sn (dotted-dashed line).

SUMMARY AND CONCLUSIONS

The systematics of the fission-like reactions of ¹²C projectiles with Y, Mo, Ag, and Sn nuclei have been studied as a function of projectile kinetic energy. The data suggest that the mechanism of these reactions, at least for the lighter products, is one which involves the continuous evolution of the system along dynamic trajectories in $\alpha_2, \alpha_3, \alpha_4$ space which lead from the fusion valley to the fission valley without necessarily passing inside the symmetric saddle point. The occurrence of such reactions is consistent with calculations indicating an increasing stabilization of the symmetric configuration in the fusion valley as the angular momentum of the system increases.

The same mechanism may also account for heavier products corresponding to near-symmetric division, particularly for the reactions with the lighter targets. However, in view of the increasing tendency towards fusion as the asymmetry of the initial collision increases and the rapid increase in the probability of fission deexcitation of a compound nucleus with increasing values of Z^2/A , the higher Z products may result predominantly from dynamic trajectories which pass inside the symmetric saddle point. It has previously been noted that the average total kinetic energies for this symmetric fission, when corrected for mass changes during the deexcitation step, are found to be in excellent agreement with the kinetic energies of symmetric fission calculated using a dynamic liquid drop model formalism.²³

ACKNOWLEDGMENT

We wish to acknowledge a number of very useful conversations with Dr. J. R. Nix. We thank K.

Geoffroy, K. Das, P. Gonthier, T. Shula, and L. Webb for their assistance in various phases of these experiments. We also appreciate the assistance of the entire staff of the Texas A&M Cyclotron Institute.

*Work supported in part by the U.S. Energy Research and Development Administration and the Robert A. Welch Foundation.

†Present address: Babcock and Wilcox Company, Lynchburg Research Center, Lynchburg, Virginia.

¹F. Hanappe, M. Lefort, C. Ngo, J. Peter, and B. Taimain, *Phys. Rev. Lett.* **32**, 738 (1974).

²J. Wilczynski, *Phys. Lett.* **47B**, 484 (1973).

³L. G. Moretto, D. Heunemann, R. C. Jared, R. C. Gatti, and S. G. Thompson, in *Proceedings of the Third International Conference on the Physics and Chemistry of Fission, Rochester, 1973* (International Atomic Energy Agency, Vienna, 1974), p. 351; L. G. Moretto, *Bull. Am. Phys. Soc.* **19**, 465 (1974).

⁴R. Kaufmann and R. Wolfgang, *Phys. Rev.* **121**, 192 (1961).

⁵G. F. Gridnev, V. V. Volkov, and J. Wilczynski, *Nucl. Phys.* **A142**, 385 (1970).

⁶A. G. Artukh, G. F. Gridnev, V. L. Mikheev, V. V. Volkov, and J. Wilczynski, *Nucl. Phys.* **A211**, 299 (1973).

⁷S. Cohen and W. J. Swiatecki, *Ann. Phys. (N.Y.)* **19**, 67 (1962).

⁸E. T. Chulick, M. N. Namboodiri, G. W. Smith, S. Munden, C. Schnatterly, and J. B. Natowitz, *Nucl. Instrum. Methods* **114**, 503 (1974).

⁹L. C. Northcliffe and R. Schilling, *Nucl. Data* **A7**, 233 (1970).

¹⁰S. B. Kaufmann, E. P. Steinberg, B. D. Wilkins, J. Unk, A. J. Gorski, and M. J. Fluss, *Nucl. Instrum. Methods* **115**, 47 (1974).

¹¹M. N. Namboodiri, J. B. Natowitz, E. T. Chulick, and K. Geoffroy (unpublished).

¹²I. Halpern and V. M. Strutinsky, in *Proceedings of the Second United Nations International Conference on the Peaceful Uses of Atomic Energy* (United Nations, Geneva, Switzerland, 1958), Vol. 15, p. 408.

¹³W. J. Swiatecki, Lawrence Berkeley Laboratory Report No. LBL-972, 1972 (unpublished); *Phys. Lett.* **4C**, 325 (1972).

¹⁴A. J. Sierk and J. R. Nix, in *Proceedings of the Third International Conference on the Physics and Chemistry of Fission, Rochester, 1973* (International Atomic Energy Agency, Vienna, 1974), Vol. II, p. 273.

¹⁵C. Y. Wong (private communication).

¹⁶R. Vandenbosch and J. R. Huizenga, *Nuclear Fission* (Academic, New York, 1973).

¹⁷R. Bass, *Nucl. Phys.* **A231**, 45 (1974).

¹⁸V. L. Businaro and S. Gallone, *Nuovo Cimento* **1**, 1102 (1955).

¹⁹S. Cohen, F. Plasil, and W. J. Swiatecki, *Ann. Phys. (N.Y.)* **82**, 557 (1974).

²⁰H. J. Krappe and J. R. Nix, in *Proceedings of the Third International Conference on the Physics and Chemistry of Fission, Rochester, 1973* (International Atomic Energy Agency, Vienna, 1974), Vol. I, p. 159.

²¹M. N. Namboodiri, E. T. Chulick, J. B. Natowitz, and R. A. Kenefick, *Phys. Rev. C* **11**, 401 (1975).

²²J. R. Nix, *Nucl. Phys.* **A130**, 241 (1969).

²³M. N. Namboodiri, J. B. Natowitz, E. T. Chulick, K. Das, and L. Webb, *Nucl. Phys.* **A252**, 163 (1975).